Process Analyzer Location and Performance Assessment for Optimal Process Monitoring

Frans W. J. van den Berg, Hans F. M. Boelens, and Age K. Smilde
Dept. of Chemical Engineering, Process Analysis and Chemometrics, University of Amsterdam, 1018 WV Amsterdam, The Netherlands

Huub C. J. Hoefsloot
Dept. of Chemical Engineering, Polymer and Process Systems, University of Amsterdam, 1018 WV Amsterdam, The Netherlands

The influence of process analyzer location and performance on plant-wide process monitoring was evaluated using five uncertainty contributions to the estimation error: measurement error/uncertainty, analysis frequency, sample size/grab error, analyzer memory effect/response correlation, and delay time. The choice of both the location and performance characteristics of different process analyzers can be evaluated using a measurability factor M, ranging from zero to one, where one indicates perfect monitoring capabilities. Due to the unifying nature of the measurability factor, this factor can be used to make a rational decision between very different process analyzers. This allows for finding optimal process analyzer configurations for existing processes or for processes in the design phase. A tubular reactor simulation model was used for the partial oxidation of benzene to maleic anhydride to demonstrate the use of the measurability factor.

Introduction

An ever-increasing number of process analyzers are implemented in the chemical industry. At the same time, the diversity in techniques suitable for harsh process conditions, such as chromatography, (near)infrared-, Raman- or (low-field) nuclear magnetic resonance spectroscopy, mass spectrometry, flow injection analysis, ultrasonic analysis, to name just a few, grows steadily (Workman et al., 1999). The implementation and operation of analytical in-process measurements is, however, still relatively expensive. (The expression "in-process" is an idiom for all off-line, at-line, on-line, in-line and non-invasive measurement techniques suited for "real-time" monitoring and/or controlling of a process.) The cost of purchase and maintenance often limits the number of analyzers that can be implemented for monitoring and/or control purposes. This naturally leads to the following three questions. What is the best location to place the limited amount of analytical instruments available? What is the best choice among the wide selection of process analyzers to monitor the process under observation? What is the added value of process analyzers as compared to more conventional, interferential measuring devices like temperature-, pressure-, flow-sensors?

In order to assess the performance of a process analyzer, we identify five contributions to characterize the process analyzer: the *analyzer dynamics*. The first contribution is the uncertainty or error encountered in every real-world measurement. The second contribution is the analysis frequency of the instrument, which determines the signal reconstruction capabilities. The third contribution is the uncertainty buildup introduced by collecting a sample of sufficient size, the so-called grab error. The fourth contribution is memory effect or correlation between successive measurements. This phenomenon is often observed in "physical" measurements like ion-selective electrodes, pH, or conductivity, where responses are correlated over time. The fifth contribution is the delay time: the time passed between taking a sample and retrieving the analysis result. Separation based composition analyzers

Correspondence concerning this article should be addressed to A. K. Smilde.

require some time to analyze the sample before the result becomes available. These five contributions are used to characterize a process analyzer, describing the way an in-process measurement observes process variables and presents them to the controllers. Additional instrumental characteristics could be considered, but the five mentioned above form a good representation of most analyzers.

In this article we model nonideal measurements for estimating the entire state of a fixed-bed tubular reactor simulation model for the catalytic partial oxidation of benzene to maleic anhydride. The state of this system is formed by the concentration and temperature profiles over the reactor tube. These state elements have to be determined from measuring one of the variables at one particular position. The optimal analyzer type and position are selected by minimizing the theoretical state estimation error in a Kalman filter. Using state estimation error as a criterion for optimization requires knowledge of the uncertainty in both the system and measurements. Many authors discussed the optimal sensor location problem using this same optimization criterion (Aidarous et al., 1975; Chen and Seinfeld, 1975; Colantuoni and Padmanabhan, 1977; Kumar and Seinfeld, 1978; Harris et al., 1980; Alvarez et al., 1981; Windes et al., 1989; Grewal and Andrews, 1993). However, these authors all work with relative simple sensors (typically temperatures), which deal mostly with measurement uncertainty and sample frequency in the optimization. For process analyzers, this is insufficient. The time delay introduced when performing an accurate gas chromatographic concentration measurement might be competing with a fast, but less accurate, spectroscopic determination. These measurement—accuracy, sample frequency, delay time, and so on—characteristics must be incorporated to fairly assess the performance of different in-process applications. We do this by incorporating all dynamics (both plant and analyzer) in one system model, creating a so-called *standard plant* (van Overschee and de Moor, 1996). We explicitly model uncertainty caused by stochastic process disturbances and analyzer characteristics, showing their impact on optimal measurement type and location from a set of realizable configurations. (If we use the word "optimal" in this article, we mean the best choice from the set of all possible process analyzers. The true "optimal analyzer" would be infinitely fast and infinitely precise which are impossible specifications for practical and real measurements.) An alternative can be found in a deterministic analyzer selection criterion (focusing on the system dynamics, not using the stochastic process uncertainty) of optimal analyzer location based on the idea of the *degree of observability* from system theory (van den Berg et al., 2000).

In the 1960s P. M. E. M. van der Grinten developed ideas to quantify the performance of measurements and control actions by approximate first-order dynamics and uncertainties (van der Grinten, 1968; van der Grinten and Lenoir, 1973). A short explanation of the theory developed by van der Grinten is given in Appendix A. He introduced two scalar values called meetbaarheids factor (measurability factor) and regelbaarheids factor (controllability factor) that quantify how well a signal can be measured and how well a disturbance can be suppressed. The ideas only found limited application outside of the Dutch engineering community, possibly due to the language barrier (Stephanopoulos, 1984). Only a few sources on this theory are available in the English language (van der Grinten, 1968; Leemans 1971; Rijnsdorp, 1986; Didden and Duisings, 1992).

The original theory of van der Grinten focuses on univariate (simplified) first-order descriptions of a process and a measurement and a fixed location. In this article we extend the five key ideas on measurement uncertainty and dynamics of van der Grinten to state estimation problems and define a measurability factor M for the multivariate case, that is, for the whole system. Moreover, we also consider the location of the analyzer in the optimization of the system's measurability.

Process analyzer location and performance assessment as presented in this article can be seen as related to other research areas such as sensor failure and data reconciliation (Darouach and Zasadzinski, 1991). However, we will not address these important issues in this article. Although an ever-increasing number of in-process analytical measurements are being installed, the implementation cost involved still does not allow them to be treated like more regular sensors. In nearly all situations, analyzers are used for key-information on process variables, and information "redundancy" from these measurements is not really an issue yet. This justifies our focus on the specific instrument characteristics for process analyzers selection and positioning.

The theory is developed on different sources of analyzer dynamics and their implementation in the Kalman filter is shown. A short description of the reactor simulation model is used as an example. The results are presented for the optimal process analyzer configuration problem (both instrument characteristics and location) for the tubular reactor, and conclusions based on the results are formulated.

Theory

Process model

Nonideal measurements of a dynamic process are modeled and, subsequently, the entire state of this system is estimated. The position of an analyzer for process monitoring or control in this article is shown in Figure 1. The process is influenced by a deterministic input (possibly modified by a regulator) and stochastic disturbances. This results in a certain process output. The analyzer measures one of the variables in the process and, together with a filter, tries to find the best estimate of the present state of the process. The estimated value is then used to adjust the regulator to achieve a desired process output. The system and measurement dynamics and uncertainties can be captured in the well-known linear, time invariant state-space format as follows (Grewal and Andrews, 1993; Gelb, 1974; Jazwinski, 1970)

$$\dot{\boldsymbol{x}}(t) = \boldsymbol{A}_c\boldsymbol{x}(t) + \boldsymbol{b}_1 u(t) + \boldsymbol{b}_2 w(t) \tag{1a}$$

$$y(t) = \boldsymbol{c}'\boldsymbol{x}(t) + v(t) \tag{1b}$$

where $\boldsymbol{x}(t)$ $(n\times 1)$ is the state of the system at time t, $\boldsymbol{A}_c$ $(n\times n)$ is the continuous time system matrix, $\boldsymbol{b}_i$ $(n\times 1)$ are input distribution vectors, $u(t)$ is the deterministic input, and $w(t)$ is the stochastic disturbance with distribution $N(0,q(t))$, where $q(t)$ is the spectral density of $w(t)$, $y(t)$ is the measurement result, $\boldsymbol{c}$ $(n\times 1)$ is the output coupling vector, and $v(t)$ is the stochastic measurement disturbance with distribu-

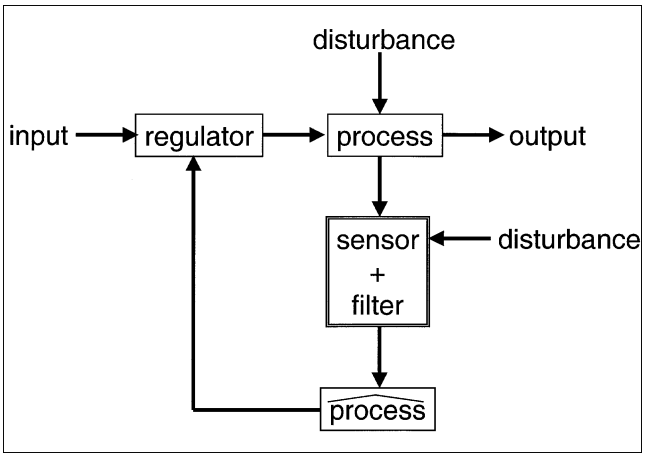

Figure 1. Position of the analyzers in process monitoring and control.

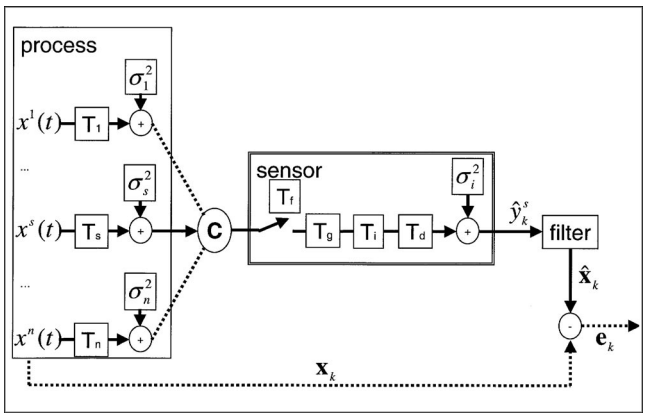

Figure 2. Sampling of one process variable in the process.

The sample is "processed" by the analyzer, and the result is used to estimate the entire system state $\boldsymbol{x}(t)$ via a filter. The goal of the in-process measurement is to minimize the estimation error $\boldsymbol{e}(t)$ over all-time t.

tion $N(0,r(t))$, where $r(t)$ is the spectral density of $v(t)$. For notational convenience, we will only treat the theory for single channel inputs and measurements (SISO); the extension to the multiple inputs/outputs (MIMO), however, is straightforward.

The discrete time solution for Eq. 1a—under zero-order hold assumption for the inputs—is $(t = k \cdot \Delta t;\ t + \Delta t = (k + 1) \cdot \Delta t)$

$$\boldsymbol{x}_{k+1} = e^{\boldsymbol{A}_c \Delta t}\boldsymbol{x}_k + \int_t^{t+\Delta t} e^{\boldsymbol{A}_c(t+\Delta t-\tau)}d\tau \boldsymbol{b}_1 u_k + \int_t^{t+\Delta t} e^{\boldsymbol{A}_c(t+\Delta t-\tau)}d\tau \boldsymbol{b}_2 w_k = \boldsymbol{A}\boldsymbol{x}_k + \boldsymbol{B}\boldsymbol{b}_1 u_k + \boldsymbol{B}\boldsymbol{b}_2 w_k \quad (2a)$$

where integral $\boldsymbol{B}$ $(n \times n)$ is implicitly defined and w_k is the variance corresponding to the spectral density $w(t)$ (Grewal and Andrews, 1993; Gelb, 1974; Jazwinski, 1970). We further assume that measurements y_k are discrete observations (with sampling time Δt) from a system through the following equation

$$y_k = \boldsymbol{c}'\boldsymbol{x}_k + v_k \quad (2b)$$

where v_k is the stochastic measurement disturbance with distribution $N(0,r_k)$ and discrete time measurement variance r_k.

In this article we adopt the concept of the *standard plant* (van Overschee and de Moor, 1996). The idea of this concept is to incorporate all dynamics (both plant and analyzer) in one system matrix $\boldsymbol{A}_c$ in Eq. 1. Augmenting the original plant system matrix with the dynamics representing the behavior of the analyzer creates the *standard plant*. The augmented states transform the true process variable selected for measurement to a new, modified variable filtered by the process analyzer dynamics. This "virtual" variable gives the signal retrieved from the analyzer. This procedure has the advantage that all dynamics present in system Eq. 1 (plant, measurement and possibly control) are captured in one model, merging all operations in one system matrix $\boldsymbol{A}_c$.

Process analyzer model

Figure 2 zooms in on the process analyzer in a monitoring or control design. One of the state variables in the process is selected for measurement. This variable can be a concentration of one of the components. The variable under observation is in Figure 2 symbolized by element $x^s(t)$ (x-signal or sampled variable) from the state vector $\boldsymbol{x}(t)$. The variable $x^s(t)$ possesses certain dynamic behavior (symbolized by T_s) and variance/amplitude (σ_s^2) due to the process disturbances. These dynamics and variances are intrinsic properties of the process. In the remainder of the article we focus on the stochastic disturbance input to the process in Eq. 1a, assuming that the deterministic input component $u(t)$ is completely known.

The analyzer "processes" the selected process variable and yields an estimated value on discrete time-points as measurement outcome y_k. This estimate is then fed to a filter that has two functions: invert the undesired signal processing by the analyzer, and estimate from this signal the present state $\hat{\boldsymbol{x}}_k$ of the system under observation. This leads to an estimation error $\boldsymbol{e}_k = \hat{\boldsymbol{x}}_k - \boldsymbol{x}_k$, and the objective is to select the measurement and filter that minimize this estimation error. An example in Appendix B will help to illustrate the theory developed in this article (van den Berg et al., 2000).

To find the optimal in-process measurement configuration for estimating the state of a process, we take six different aspects into consideration. The first one is the selection of the process/state variable and location to be sampled. This selection is guided by the amount of information that a vari-

able contains on the dynamics of the process under investigation, the availability of a suitable in-process instrument for monitoring in "real-time" that variable at that location, and the matching of the process dynamics and analyzer dynamics. The variable selection is achieved by defining the appropriate measurement vector $\boldsymbol{c}$ in Eq. 2b.

The second aspect is measurement uncertainty σ_i^2 (Figure 2) present in all physical and analytical measurements. Uncertainty in the analyzer outcome is approximated by the true quantity $y_k(t) = \boldsymbol{c}'\boldsymbol{x}_k$ plus additive white noise v_k with known distribution, typically determined during the calibration procedure or supplied by the instrument vendor

$$\hat{y}_k = y_k + v_k \qquad v_k = N\left(0, \sigma_i^2\right) \tag{3}$$

which is similar in form as the system measurement Eq. 2b.

The second source of error is the sampling frequency of the instrument, the error introduced by making discrete observations on the continuous time process with continuous time disturbances. This analyzer characteristic is symbolized by the time interval between successive sample T_f (where the sample frequency is $1/T_f$, Figure 2), and its impact on signal reconstruction is again illustrated in Figure 3. We assume equidistant samples where the basis for switching from continuous time in Eq. 1 to discrete time in Eq. 2 is the period Δt between two successive measurements. Therefore, this parameter determines the time-period over which stochastic disturbance $w(t)$ in Eq. 1 is free to alter the system state before a new observation is done. The uncertainty about the state can only be reduced when this new measurement becomes available and a new state estimate is made. For many instruments (such as spectrophotometers), there is a trade-off possible between the sample frequency and the measurement uncertainty in Eq. 2. If more time is taken per analysis, thereby increasing the signal-to-noise ratio, the measurement error can be reduced, at the cost of less frequent measurement outcomes.

The fourth phenomenon is introduced by sample size or grab size. This component to the analyzer dynamics is named T_g (Figure 2). As an example, think of a spectrophotometer averaging several spectra in a certain period of time to reduce the noise contribution in Eq. 2b. The mean spectrum with better signal-to-noise ratio can then be used to compute a concentration.

The expected value of a measurement taken over a short period of time is the average value over that time period. This expected value becomes available once the entire sample period has passed. Under the assumption that sampling or grab-time is short compared to the dominant time constants of the system, we associate the measurement response with the mean-time on this sampling time interval. Therefore, we penalize the integration or sample time with a time

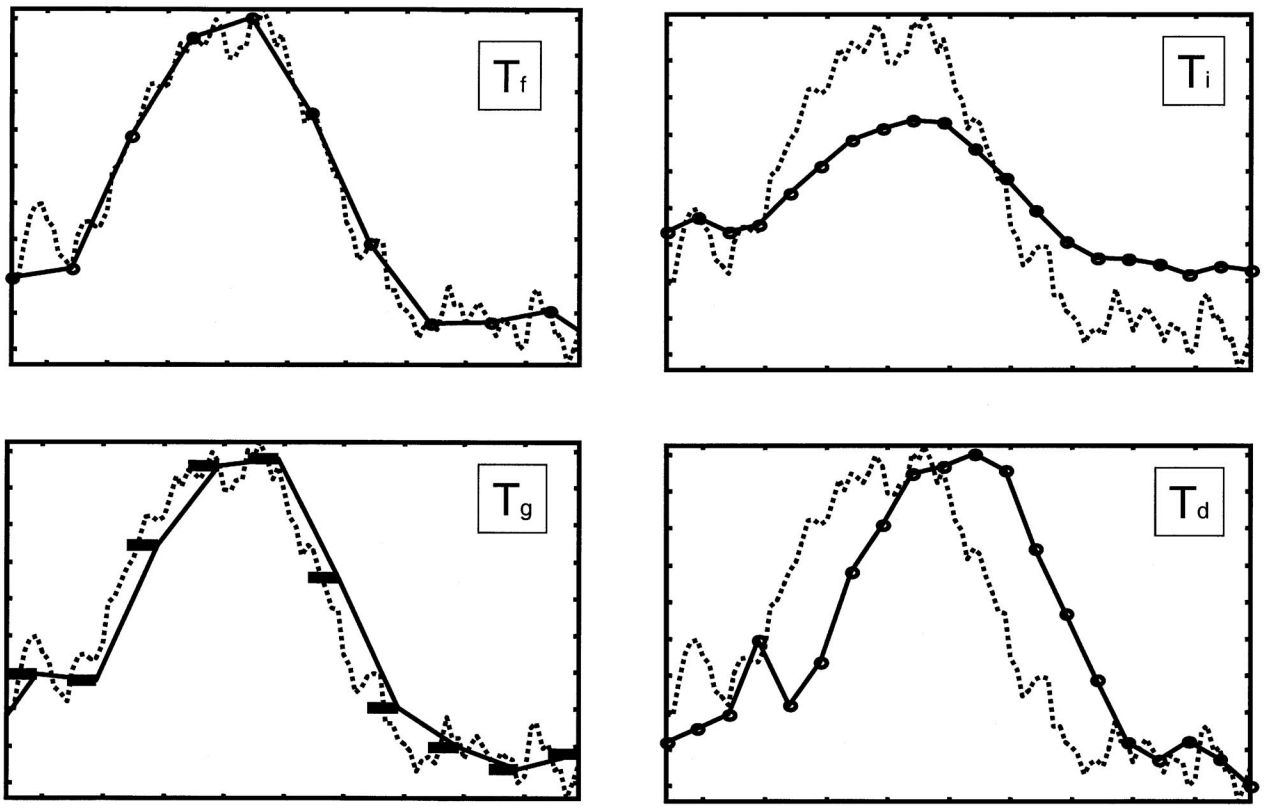

Figure 3. Effect of different process analyzer dynamics contributions on the observation of a variable for the outer world.

T_f sampling frequency, T_g grab or sample, T_i sensor response correlation and T_d response delay. Markers indicate measurement points/trajectories, (..) is the true signal and (−) is the sensor response.

delay of $T_g/2$ seconds. The effect of sample time or grab-size on signal reconstruction is illustrated in Figure 3. It is impossible to represent pure delays in the state-space time domain notation in Eq. 1. A good approximation of pure delay for the problems presented in this article turns out to be a third-order Padé approximation, shown here in Laplace domain notation (Stephanopoulos, 1984)

$$\hat{y}(s) = e^{-\frac{T_g}{2}s} y(s) + v(s) \approx \frac{-s^3 + \frac{24}{T_g}s^2 - \frac{120}{T_g^2}s + \frac{240}{T_g^3}}{s^3 + \frac{24}{T_g}s^2 + \frac{120}{T_g^2}s + \frac{240}{T_g^3}} y(s) + v(s) \quad (4)$$

The concrete implementation of time delay in the state-space time domain for the *standard plant* concept is illustrated by the example in Appendix B.

The fifth component in process analyzer performance is the correlation between successive measurements. In many instruments there is significant carry-over in the detector/signal response from one measurement to the next (such as pH ion selective electrodes or temperature dependent resistors), and this "memory effect" can be modeled explicitly. We assume exponentially first-order correlation of the autoregressive form

$$\hat{y}_{k+1} = e^{-1/T_i}\hat{y}_k + \sqrt{1-\left(e^{-1/T_i}\right)^2}\, v_k \quad v_k = N\left(0, \sigma_i^2\right) \quad (5)$$

where T_i is the correlation time between successive measurements (Figure 2) and the uncertainty v_k is scaled to have equal magnitude as the uncertainty contribution in Eq. 3. The effect of sensor response correlation on signal reconstruction is illustrated in Figure 3. As can be seen, it is effectively a convolution between the instrument dynamics and the true underlying variable. The practical implementation is again shown in the example in Appendix B.

The last component describing the performance of an in-process instrument is the delay time between sampling and the release of the result (T_d in Figure 2). A frequently encountered example of an analyzer with a significant time delay is a gas chromatograph for concentration measurements, where the different components in a sample first have to be physically separated before the analysis results can be determined. We again use a Padé approximation—similar to the one for sample size in Eq. 4—to approach pure-time delay

$$\hat{y}(s) = e^{-T_d s} y(s) + v(s) \approx \frac{-s^3 + \frac{12}{T_d}s^2 - \frac{60}{T_d^2}s + \frac{120}{T_d^3}}{s^3 + \frac{12}{T_d}s^2 + \frac{60}{T_d^2}s + \frac{120}{T_d^3}} y(s) + v(s) \quad (6)$$

To stress the importance of the dynamics of in-process analyzers, Figure 4 shows the "time-profile" of a measurement. Only after a period equal to the delay time T_d plus half the sample period T_g will the results become available, while the sample frequency T_f determines how often a measurement outcome is retrieved. Optimal selection of instrument type and location must guarantee that sufficient information is left in the measurements to make a good "real-time" estimate of the state of the system.

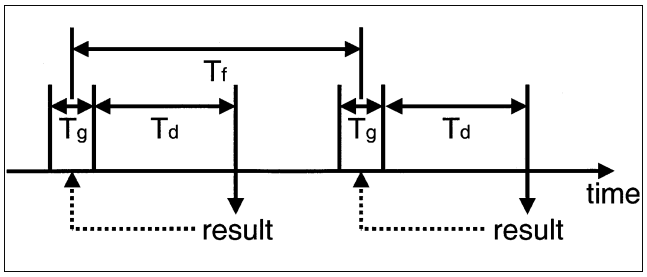

Figure 4. Time schedule for an in-process measurement. (↔) indicate the different time spans, (..) designate the time-point a measurement result is connected with.

State estimation with a Kalman filter

The filter used for state estimation of the *standard plant* model—as depicted in Figures 1 and 2—in this article is the well-known Kalman filter (Grewal and Andrews, 1993; Gelb, 1974; Jazwinski, 1970). It consists of two parts:

(i) The state estimation time update (known as *a priori* estimate $\hat{\boldsymbol{x}}_k^-$) between two successive measurements k and $k+1$, separated Δt s

$$\hat{\boldsymbol{x}}_{k+1}^- = \boldsymbol{A}\hat{\boldsymbol{x}}_k^+ + \boldsymbol{B}\boldsymbol{b}_1 u_k \quad (7a)$$

$$\boldsymbol{P}_{k+1}^- = \boldsymbol{A}\boldsymbol{P}_k^+\boldsymbol{A}' + \boldsymbol{Q}_k \quad (7b)$$

(ii) The state estimate measurement update/correction (known as *a posteriori* estimate $\hat{\boldsymbol{x}}_k^+$) using the measurement result at point $k+1$

$$\boldsymbol{k}_{k+1} = \boldsymbol{P}_{k+1}^-\boldsymbol{c}\left(\boldsymbol{c}'\boldsymbol{P}_{k+1}^-\boldsymbol{c} + \boldsymbol{r}_k\right)^{-1} \quad (8a)$$

$$\hat{\boldsymbol{x}}_{k+1}^+ = \hat{\boldsymbol{x}}_{k+1}^- + \boldsymbol{k}_{k+1}\left(y_{k+1} - \boldsymbol{c}'\hat{\boldsymbol{x}}_{k+1}^-\right) \quad (8b)$$

$$\boldsymbol{P}_{k+1}^+ = \left(\boldsymbol{I} - \boldsymbol{k}_{k+1}\boldsymbol{c}'\right)\boldsymbol{P}_{k+1}^- \quad (8c)$$

where $\boldsymbol{k}_{k+1}$ is the Kalman filter gain, $\boldsymbol{P}_{k+1}^+$ is the theoretical *a posteriori* estimation error covariance matrix, and $\boldsymbol{Q}_k$ is the positive semi-definite uncertainty distribution covariance matrix

$$\boldsymbol{Q}_k = \int_t^{t+\Delta t} e^{\boldsymbol{A}_c(t+\Delta t-\tau)}\boldsymbol{b}_2 q(\tau)\boldsymbol{b}_2' e^{\boldsymbol{A}_c'(t+\Delta t-\tau)} d\tau \quad (9)$$

The matrix $\boldsymbol{Q}_k$ represents the contribution of the system disturbance $w(t)$ in Eq. 1 on the overall state estimation error in Eq. 7. Uncertainty $w(t)$—with a spectral density of $q(t)$—is injected in the process with a system matrix $\boldsymbol{A}_c$. Uncertainty in Eq. 2a continuously builds up over the time-period

t to $t+\Delta t$, the time between two discrete measurements in Eq. 2b. At these discrete measurement time-points, all uncertainty can—for the hypothetical case of perfect measurements—be removed, but not before these points.

The Kalman filter as presented in Eqs. 7 and 8 is an unbiased, minimum variance and consistent estimator for the linear (or linearized) system in Eq. 1. If the system is observable and controllable, and if $\boldsymbol{Q}_k$, r_k and $\boldsymbol{A}$ are bounded, the filter is asymptotically stable, meaning that all the eigenvalues of the matrix $\boldsymbol{A}-\boldsymbol{k}_k\boldsymbol{c}'$ fall within the unit circle.

Notice that in the approach taken in this article, the role of $\boldsymbol{Q}_k$—the constant term in the difference equation for the theoretical estimation error $\boldsymbol{P}_k$ in Eq. 7b—is somewhat different than the one encountered in many other studies (Aidarous et al., 1975; Chen and Seinfeld, 1975; Colantuoni and Padmanabhan, 1977; Kumar and Seinfeld, 1978; Harris et al., 1980; Windes et al., 1989). Here, we give $\boldsymbol{Q}_k$ the role of describing the uncertainty propagation in the system for a period Δt between two measurements, since this is of importance for the optimal process analyzer location problem addressed in this research. Known uncertainties for the system parameters in $\boldsymbol{A}$ can also be accounted for by placing the appropriate values in the system uncertainty covariance matrix $\boldsymbol{Q}_k$. In many applications this is done by (post-run) analysis, "tuning" the diagonal elements in $\boldsymbol{Q}_k$ to create a better fit between some reference values and the Kalman-predictions. In this article, however, we give guidelines for an analyzer type and location selection in an early design stage of a process, which obviously excludes the use of post-run information. Known uncertainty in the system parameters can however be included in the system error matrix $\boldsymbol{Q}_k$ if available. Instrument selection and location are optimized by minimizing a sensible norm of the expected estimation error $\boldsymbol{P}_k$ given by the algorithm in Eqs. 7 and 8. For linear time invariant systems, this theoretical estimation error can be calculated *a priori* by implementing Eqs. 7b, 8a, and 8c. This means that the optimal analyzer type and location can be determined without any form of process simulations.

Measurability factor

From Eq. 9, we notice that—for a stable system matrix $\boldsymbol{A}_c$—there is an upper bound on the system uncertainty covariance matrix by $\boldsymbol{Q}_k$ for $\Delta t \rightarrow \infty$ (the covariance matrix of uncertainty propagation through the system). This value for Q_k corresponds with the maximum uncertainty in knowledge about the state of the process, corresponding to the situation where no measurements whatsoever are performed. When an analyzer/filter-combination is used to do an estimate, some of the uncertainty about the process state will be removed. The remaining uncertainty contribution after a measurement update is represented by the estimation error covariance matrix $\boldsymbol{P}_k$ in Eq. 8c. The performance of an analyzer/filter pair can be judged by the size of this uncertainty residual.

Using this upper bound we can define a performance index for a particular in-process measurement configuration (Appendix A)

$$M^2 = \frac{\text{trace}(\boldsymbol{Q}_k) - \text{trace}(\boldsymbol{P}_k)}{\text{trace}\ (\boldsymbol{Q}_k)} \tag{10}$$

We will call the square root of this quantity the measurability factor. M can vary between 0 and 1, where 1 means perfect knowledge about the state of the system after a measurement is taken (all uncertainty has been removed by the measurement and state estimate), while 0 indicates that a particular measurement configuration supplies no information about the state of the process. (For an extremely poor choice of analyzer, the trace of $\boldsymbol{P}_k$ could theoretically exceed the trace of $\boldsymbol{Q}_k$, giving a negative result for Eq. 10 and a negative value for the measurability factor M.) The best analyzer type and location is taken as the one maximizing the measurability factor M. If the system is unstable there is no upper bound on the error covariance matrix. The criterion to judge the performance of the analyzer/filter combination is the trace of the estimation error covariance matrix $\boldsymbol{P}_k$ and the system uncertainty $\boldsymbol{Q}_k$. This norm corresponds to the sum of estimation error variances, thereby giving variances for all variables equal weight.

All process variables from one measurement will be estimated, and equal weight will be placed on all errors through the trace criterion in Eq. 10. If installing more analyzers is feasible or if appropriate information is available, alternative (weighted) selection criteria can be introduced placing heavier penalties on mismatch for certain process variables. There is no problem in introducing these alternative criteria in the proposed procedure of optimal instrument selection and positioning.

Tubular Reactor Model

The theory on analyzer selection developed in this article is illustrated with a simulation model of a fixed-bed tubular reactor for the production of maleic anhydride by partial oxidation of benzene (van den Berg et al., 2000; Ramirez and Calderbank, 1977; Wohlfahrt and Emig, 1980). Three exothermic, irreversible gas-phase reactions take place on a solid V_2O_5-MoO_3-P_2O_5 catalyst particles packed in a 1 in. diameter tube

$$C_6H_6 + 4O_2 \xrightarrow[k_1]{} C_4H_2O_3 + CO + CO_2 + 2H_2O \tag{11a}$$

$$C_6H_6 + 6O_2 \xrightarrow[k_2]{} 3CO + 3CO_2 + 3H_2O \tag{11b}$$

$$C_4H_2O_3 + 2O_2 \xrightarrow[k_3]{} 2CO + 2CO_2 + H_2O \tag{11c}$$

Reaction 11a is the desired path for the formation of maleic anhydride—the product—from benzene. Reactions 11b and 11c represent the undesired burning of reactant and product, respectively. The feedstream to the reactor is air mixed with approximately 0.9% (v/v) benzene. Because of the oxygen excess in the feed, all reactions are assumed to be pseudo first-order in the limiting reactant.

The two mass balances used in the model are molar-flow benzene F_B ($\text{mol}\cdot\text{s}^{-1}$) and molar-flow maleic anhydride F_{MA} ($\text{mol}\cdot\text{s}^{-1}$) in the fluid phase stream. The partial differential equations are given by Eqs. 12a and 12b (t denotes time; z indicates axial position in the reactor; υ is linear gas velocity

of 2.48 $m \cdot s^{-1}$; D_{eff} is effective mass diffusion coefficient)

$$\frac{\partial F_B(t,z)}{\partial t} = -v\frac{\partial F_B(t,z)}{\partial z} + D_{\text{eff}}\frac{\partial^2 F_B(t,z)}{\partial z^2} - k_1(t,z)F_B(t,z) - k_2(t,z)F_B(t,z) \quad (12a)$$

$$\frac{\partial F_{MA}(t,z)}{\partial t} = -v\frac{\partial F_{MA}(t,z)}{\partial z} + D_{\text{eff}}\frac{\partial^2 F_{MA}(t,z)}{\partial z^2} + k_1(t,z)F_B(t,z) - k_3(t,z)F_{MA}(t,z) \quad (12b)$$

Two heat balances are included in the simulation, namely, the temperature of the fluid-phase T_f (K) and the temperature of the stagnant solid-phase catalyst T_s (K). The corresponding (partial) differential equations are shown in Eqs. 12c and 12d (k_{eff} is effective heat diffusion coefficient, $U_{f\text{-}w}$ is the fluid phase-wall heat-transfer coefficient; $U_{s\text{-}f}$ is the solid-phase fluid-phase heat-transfer coefficient, T_w is the reactor-wall temperature; $c_s\Delta H_x$ is a reaction enthalpy coefficient)

$$\frac{\partial T_f(t,z)}{\partial t} = -v\frac{\partial T_f(t,z)}{\partial z} + k_{\text{eff}}\frac{\partial^2 T_f(t,z)}{\partial z^2} - U_{f-w}\big(T_f(t,z)-T_w\big) - U_{s-f}\big(T_s(t,z)-T_f(t,z)\big) \quad (12c)$$

$$\frac{dT_s(t,z)}{dt} = -U_{s\text{-}f}\big(T_s(t,z)-T_f(t,z)\big) + c_s\Delta H_1 k_1(t,z)F_B(t,z) + c_s\Delta H_2 k_2(t,z)F_B(t,z) + c_s\Delta H_3 k_3(t,z)F_{MA}(t,z) \quad (12d)$$

Figure 5 shows the steady-state concentration and temperature profiles over the reactor tube for three different benzene feeds. The boundary conditions used in the calculations are $F_B(t,0) = [\text{feed}]\ \text{mol}\cdot\text{s}^{-1}$, $F_{MA}(t,0) = 0\ \text{mol}\cdot\text{s}^{-1}$ and $T_f(t,0) = 733$ K. Diffusion effects at the entrance and exit are neglected.

The nonlinear partial differential equation system in Eq. 12 is rewritten in a linear, finite dimensional state-space reactor model (van den Berg et al., 2000). The first step is to divide the reactor length into m equidistant segments indicated by z_i, where z_0 is the reactor entrance. For every grid-point z_i, we define four (partial) differential equations from Eq. 12. In the next step, the first-and second-order differential terms in the partial differential equations on every grid-point are approximated by second-order upwind and central differential terms. After this step, the original reactor model is transformed into a set of $n = 4\times m$ ordinary differential equations, two mass and two heat-balances on all m grid-point over the reactor length ("method of lines" approximation). The last step is to linearize all nonlinear terms in the reactor

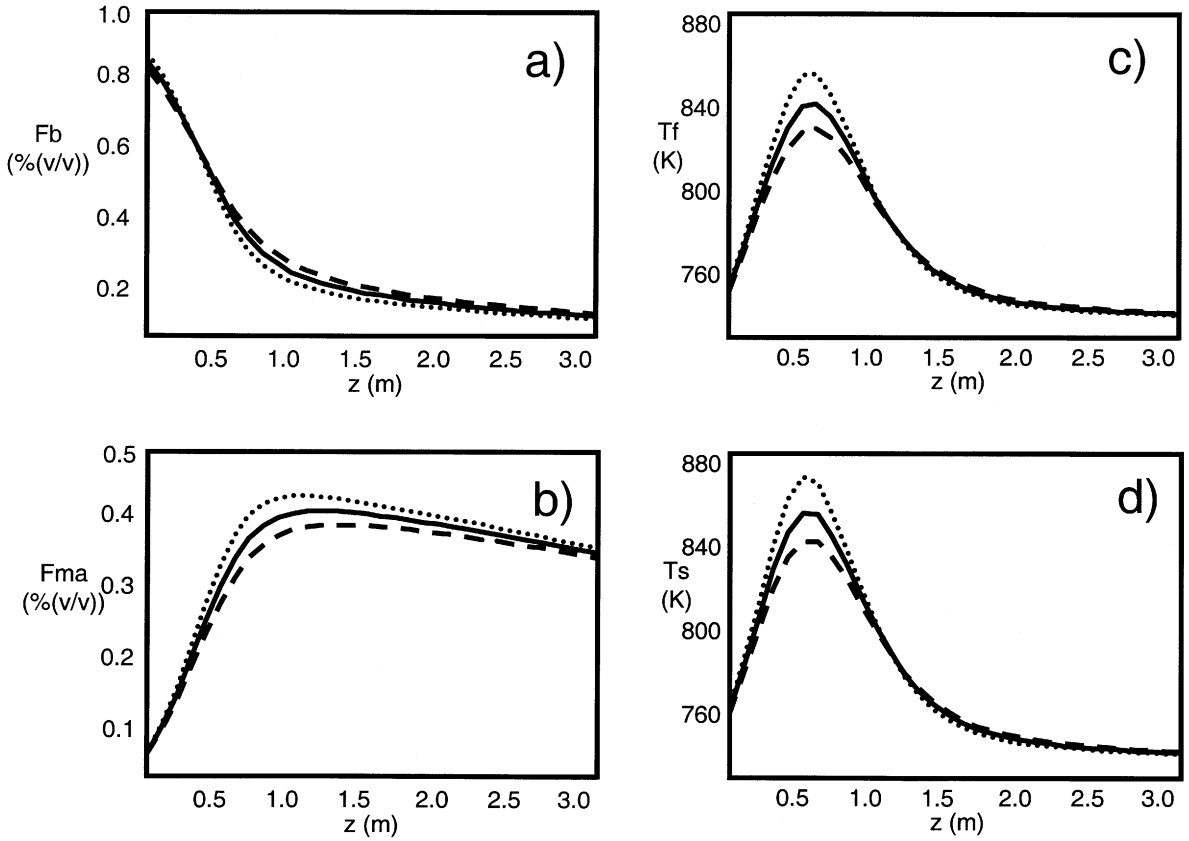

Figure 5. (a) Molar flow benzene; (b) molar flow maleic anhydride; (c) fluid phase temperature; (d) solid phase temperature, benzene feed 0.900 (–), 0.0873 (..) and 0.927% (v/v) (– –).

model. This is done by a first-order Taylor-series approximation.

After these modifications, the original reactor model is transformed into n linear time invariant ordinary differential equations. They can then be organized in a state-space model as shown in Eq. 1a. The state vector is organized in an alternating fashion $\boldsymbol{x}(t)=[F_B(t,z_1),\ F_{MA}(t,z_1),\ T_f(t,z_1),\ T_s(t,z_1),\ F_B(t,z_2),\ \ldots,\ T_s(t,z_m)]'$. The band diagonal dynamic coefficients matrix $\boldsymbol{A}_c$ has appropriate constants connecting the n linear differential equations for successive grid points. In our reactor model, both the deterministic input $u(t)$ and the stochastic input $w(t)$ is benzene concentration in the feedstream. This system for our reactor model is asymptotically stable.

To simulate analyzers in the reactor, the system measurement Eq. 1b is used. All the components of the analyzer dynamics are included in the augmented system matrix $\boldsymbol{A}_c$ in accordance with the *standard plant* concept.

Results

To study the effect of process analyzer uncertainty and dynamics, we introduce three kinds of measurements in our reactor simulation model presented in the previous paragraph (Skoog, 1985; Pallás-Areny and Webster, 1991). The first instrument is a fast, but relatively inaccurate, spectroscopic measurement of the benzene (B) or maleic anhydride (MA). The second analyzer is a fast gas chromatographic (GC) measurement of benzene or maleic anhydride. For this analyzer, accuracy is increased at the cost of introducing delay-time necessary to physically separate the different components in instrument. The third measurement is a thermal resistor sensor for the solid or fluid-phase temperature in the reactor tube. This is an example of an instrument having significant correlation in the response. The specification of each instrument is specified in Table 1.

The disturbance on the system is a 10% fluctuation of the nominal benzene feed-flow of 0.9% (v/v). Using Eqs. 7, 8 and 9, the theoretical estimation error for the different instruments is computed. The task of the Kalman filter is to estimate from the measurement outcome all state variables $\boldsymbol{x}(t)$ in the reactor tube in Eq. 13. The measurability factors for the three process analyzers, specified in Table 1, placed at different locations in the reactor tube are shown in Figure 6.

From Figure 6 and Table 1, we learn that the best performance for monitoring the benzene/maleic anhydride reactor is achieved by analyzer (a)—the fast but less accurate spectroscopic analyzer—measuring maleic anhydride at $z=$ 0.6–0.7 m. Instrument (a) also gives a good performance for benzene concentration analysis near the entrance, which is close to the source of disturbance for the reactor model, namely fluctuation in the benzene feed. The second observation is that estimation of the reactor state using analyzer (b) performs poorly for both benzene and maleic anhydride analysis. The delay time T_d of 5 s for this GC-analysis is simply too long for this process and the measurement therefore contains hardly any information for real-time monitoring the system state. The third sensor (c) in the location $z=$ 0.4–0.7—sampling temperature of fluid or solid phase in the

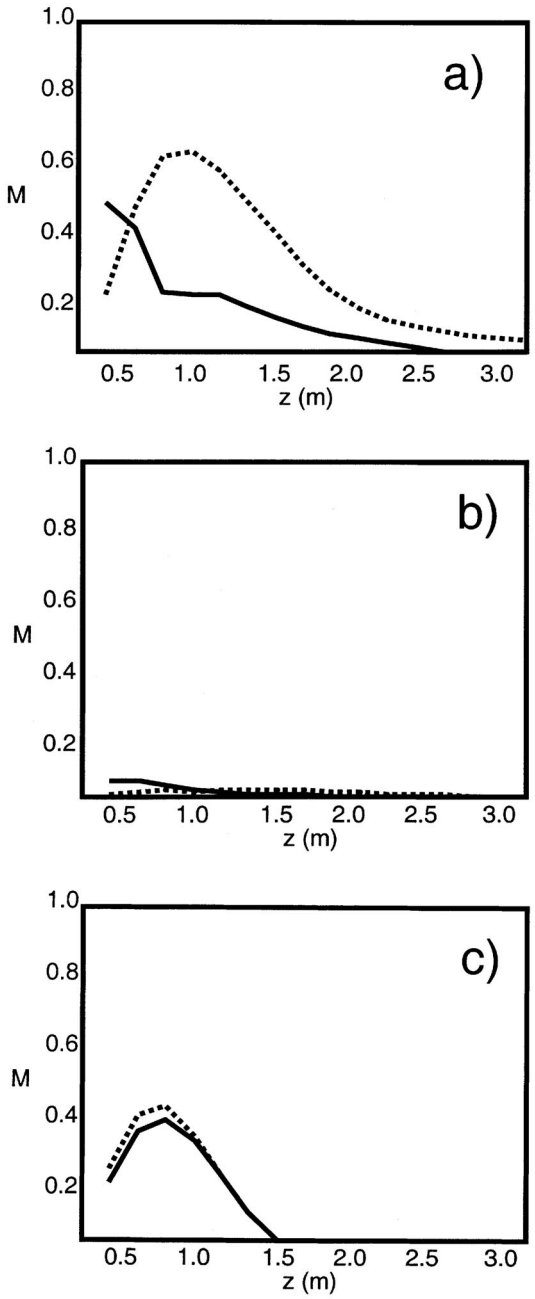

Figure 6. Measurability factor *M* for different analyzer configurations at different locations in reactor tube.

(a) spectrometer for B (–) and MA (..); (b) GC B (–) and MA (..); (c) temperature fluid (–) and solid (..) phase.

Table 1. Specifications of Three Analyzers Used in Tube Simulation Studies

Analyzer	σ_1	T_g^*	T_i^*	T_f^*	T_d^*
(a) Spectrometer	B : 0.045%(v/v) MA: 0.030%(v/v)	—	—	0.05 s	—
(b) GC	B : 0.014%(v/v) MA: 0.09%(v/v)	—	—	5.00 s	5.00 s
(c) Thermal resistor	1.5 K	—	3.0 s	0.05 s	—

* —Means no significant contribution for the overall performance of this type of analyzer.

reactor tube—is a reasonable alternative for the use reactor state estimation, although not as good as the concentration measurement with analyzer (a).

If we look at Figure 6, together with the nominal reactor profiles plotted in Figure 5, we can draw some additional conclusions. The first one is that none of the instruments perform well in the last part of the reactor tube. Not much information on the dynamic behavior of the reactor system is available in the last half of the system, as is to be expected. A second observation is that the rather extreme "hot-spot" plays a crucial role in the location. Temperature measurements are clearly dominated by its location, while the concentrations are indirectly influenced by the "negative feedback" for the exothermic oxidation of benzene, as can be observed in Figure 5a. Another observation is that all optimal positions have slightly moved towards the reactor entrance, as compared to deterministic selection criteria for optimal measurement location (van den Berg et al., 2000). Two reasons can be identified: the interaction of analyzer and reactor dynamics, and the fact that the only disturbance for this particular example system was selected to be the uncertainty in the benzene feed at the reactor entrance. If alternative disturbances, possibly taking place at different positions in the reactor tube, were to be included in the process model, the optimal measurement location might be altered.

Conclusions

It has been shown that the dynamic behavior of a process analyzer plays an important role in the selection of the optimal in-process measurement type and location. Six contributions that are needed to specify the in-process analyzer performance have been identified: analyzer location, uncertainty σ_i^2, sample frequency T_f, sample/grab size T_g, response correlation T_i, and delay time T_d. Other important components in the success or failure of the process state estimation problem are the dynamics T_s and amplitude σ_s^2 of the process variable selected for measurement.

In our case study—partial oxidation of benzene to maleic anhydride in a tubular reactor—the best analyzer is a fast spectroscopic measurement of the product and, to a lesser extent, the reactant. Gas chromatographic measurement of neither reactant nor product performed well, due to the relative large delay time associated with this instrument. Temperature measurement of fluid and solid phase also performed well in the "hot-spot" region of the reactor tube.

The approach as formulated in this article—including all process analyzer relevant dynamics in the so-called *standard plant*, and using the theoretical estimation error to compute the measurability factor—can serve to optimize new in-process measurement implementations. This optimization for analyzer type and position can be done in an early ("drawing board") stage of the process design cycle. By using analyzer specifications, retrieved from, for example, instrument vendors, analytical chemistry departments, or earlier experiences, and a model of the process, the theory developed in this article makes it possible to determine the feasibility of process state estimation and monitoring tasks. The measurability factor M is a convenient scalar number to compare different in-process measurement configurations. The tools formulated in this article can be used to investigate the potential of in-process measurements.

Literature Cited

Aidarous, S. E., M. R. Gevers, and M. J. Installé, "'Optimal sensors' Allocation Strategies for a Class of Stochastic Distributed Systems," *Int. J. of Control*, **22**, 197 (1975).

Alvarez, J., J. A. Romagnoli, and G. Stephanopoulos, "Variable Measurement Structures for the Control of a Tubular Reactor," *Chem. Eng. Sci.*, **36**, 1695 (1981).

Bryson, A. E., and D. E. Johansen, "Linear Filtering for Time-Varying Systems Using Measurements Containing Colored Noise," *IEEE Trans. on Automatic Control*, **1**, 4 (1965).

Chen, W. H., and J. H. Seinfeld, "Optimal Location of Process Measurements," *Int. J. of Control*, **21**, 1003 (1975).

Colantuoni, G., and L. Padmanabhan, "Optimal Sensor Locations for Tubular-Flow Reactor Systems," *Chem. Eng. Sci.*, **32**, 1035 (1977).

Darouach, M., and M. Zasadzinski, "Data Reconciliation in Generalized Linear Dynamic Systems," *AIChE J.*, **37**, 193 (1991).

Didden, C., and J. Duisings, "On-Line Measurement of a Liquid Reactor Feed with a Mass Spectrometer," *Process Control and Quality*, **3**, 263 (1992).

Gelb, A., *Applied Optimal Estimation*, MIT Press, Cambridge (1974).

Grewal, M. S., and A. P. Andrews, *Kalman Filtering*, Prentice Hall, Englewood Cliffs (1993).

Harris, T. J., J. F. MacGregor, and J. D. Wright, "Optimal Sensor Location with Application to a Packed Bed Tubular Reactor," *AIChE J.*, **26**, 910 (1980).

Jazwinski, A. H., *Stochastic Process and Filtering Theory*, Academic Press, San Diego (1970).

Kumar, S., and J. H. Seinfeld, "Optimal Location of Measurements in Tubular Reactors," *Chem. Eng. Sci.*, **33**, 1507 (1978).

Leemans, F. A., "Selection of an Optimal Analytical Technique for Process Control," *Analytical Chemistry*, **43**(11), 36A (1971).

Pallás-Areny, R., and J. G. Webster, *Sensors and Signal Conditioning*, Wiley, New York (1991).

Ramirez, J. F., and P. H. Calderbank, "The Oxidation of Benzene in Packed Catalyst Beds," *Chem. Eng. J.*, **14**, 49 (1977).

Rijnsdorp, J. E., "The Contribution of Quality Aspects to Process Control," *Analytica Chimica Acta*, **190**, 33 (1986).

Skoog, A. S., *Principles of Instrumental Analysis*, Sauders College Publishing, Philadelphia, PA (1985).

Stephanopoulos, G., *Chemical Process Control*, Prentice Hall, Englewood Cliffs (1984).

van den Berg, F. W. J., H. C. J. Hoefsloot, H. F. M. Boelens, and A. K. Smilde, "Selection of Optimal Sensor Position in a Tubular Reactor Using Robust Degree of Observability Criteria," *Chem. Eng. Sci.*, **55**, 827 (2000).

van der Grinten, P. M. E. M., "Uncertainty in Measurement and Control" *Statistica Neerlandica*, **22**, nr. 1, 43 (1968).

van der Grinten, P. M. E. M., and J. M. H. Lenoir, "Statistische Procesbeheersing," *Spectrum*, Utrecht, The Netherlands (1973).

van Overschee, P., and B. de Moor, *Subspace Identification for Linear Systems*, Kluwer Academic Publishers, Norwell, MA (1996).

Windes, L. C., A Cinar, and W. H. Ray, "Dynamic Estimation of Temperature and Concentration Profiles in a Packed Bed Reactor," *Chem. Eng. Sci.*, **44**, 2087 (1989).

Wohlfahrt, K., and G. Emig, "Compare Maleic Anhydride Routes," *Hydrocarbon Proc.*, **83** (June 1980).

Workman, J., et al., "Process Analytical Chemistry," *Analytical Chemistry*, **12**, 121R (1999).

Appendix A

In this Appendix we give an introduction to the ideas as presented by P. M. E. M. van der Grinten on optimization of measurements and control schemes (van der Grinten, 1968; van der Grinten and Lenoir, 1973). We have changed some of the notations used in the original work in order to create a closer parallel with the work presented here.

Controlling is intervening in a situation on the basis of measurements (van der Grinten, 1968). Three possible sources for lack of controller performance can be identified in this definition: (I) The measurement may be in error due

to sensor inaccuracies and sluggishness. (II) The intervention may lose its effectiveness through over-determinacy or dynamically unfavorable regulator behavior. (III) The static and dynamic characteristics of the system under control are insufficiently known. If a measurement is used for control, the accuracy and speed with which the result becomes available are of equal importance. If time is lost in the measurement, or sampling intervals are long, the systems status may have changed without this appearing in the sensor response. Intervention made on such a basis can never be fully correct.

Three dynamic operations are identified for the measured signal (denoted $w(t)$): the sample time or frequency T_f, the averaging or grab-size time T_g, and the delay time T_d, needed to condition and process the sample (Figure 4). A measurement error $v(t)$ is superimposed on the result. In many practical applications a reconstruction filter is used to minimize error $e(t)$ between the sensor outcome and the true value. In evaluating the efficiency of the estimator, only variations in the measured quantity $w(t)$ and the measuring error $v(t)$ are considered (systematic errors are not included). The definition A1 is used to determine optimum efficiency

$$m^2 = \frac{\sigma_w^2 - \sigma_e^2}{\sigma_w^2} \tag{A1}$$

where m denotes the measurability factor ("meetbaarheids factor"), indicating what part of the signal is actually measured under optimal conditions ($m = 1$ is a perfect reconstruction; $m = 0$ means no information at all).

Completely analogous we can define an efficiency factor for the control structure, again focusing on the changes of the variable about their nominal value. Variable $w(t)$ now represents the equivalent disturbance (summed effect of all disturbances on the process) in the point immediately before the measurement location. The goal of stabilizing control is to minimize the resulting error output $e(t)$. The controller efficiency is now derived as

$$r^2 = \frac{\sigma_w^2 - \sigma_e^2}{\sigma_w^2} \tag{A2}$$

where controllability factor ("regelbaarheids factor") r indicates the extent to which disturbances can be suppressed. Notice that r can never exceed m. This means that besides, for example, slugguishness of the controller itself, the sensor performance can dominate the overall control performance.

Dynamics of stationary signal or time series $w(t)$ can be characterized by their auto-correlation function, which for many physical systems can be approximated by Markov processes

$$\varphi_{ww}(\tau) = E[w(t)w(t+\tau)] \approx \sigma_w^2 e^{-\tau/T_w} \quad \varphi_{ww}(0) = \sigma_w^2 \tag{A3}$$

Equation A3 can be seen as a prediction curve, characterized by the variance/amplitude σ_w^2 and the correlation time T_w. The latter can be estimated already during the design stage by computing the largest time constant of the expected disturbances.

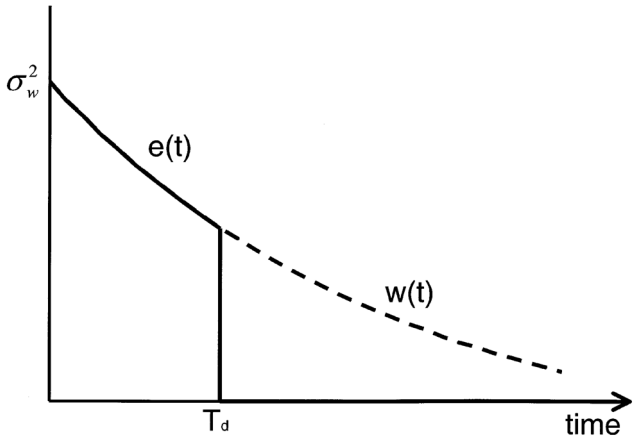

Figure A1. Role of delay time on the controller performance.

To achieve good control the overall delay-time (sum of sensor and controller delay) must be smaller than the disturbance time constant: $T_d < T_w$. This is illustrated in Figure A1 for the case of optimal control. A disturbance $w(t)$ will emerge as output error $e(t)$ until time equals $t = T_d$, after which the error is compensated for by the controller. From this observation and Eq. A2, a controllability factor due to delay-time is deduced.

$$r_d = e^{-T_d/T_w} \tag{A4a}$$

For all other combinations to the overall measurement and control uncertainty, similar equations can be derived. These are often simplifications of more complicated, statistically more thorough descriptions. Only the final results are presented here. For details on derivations, more complicated auto-correlation functions, and process disturbances we refer to van der Grinten (1968). The contribution of sampling frequency is given by

$$m_f = e^{-T_f/2T_w} \tag{A4b}$$

The factor $1/2T_f$ stems from the notion that information at the moment of sampling is complete, but, immediately before the next sampling, the information is obsolete by a time equal to T_f. Similar reasoning leads to an equation for the sample size error

$$m_g = e^{-T_g/2T_w} \tag{A4c}$$

Formulas can be derived for the measurement error with sensor error correlation T_v and the inverse controller response with inversion time T_{in}

$$m_n \approx 1 - \frac{\sigma_v}{\sigma_w}\sqrt{\frac{T_v}{T_w}} \tag{A4d}$$

$$r_{in} = \frac{1 - T_{in}/T_w}{1 + T_{in}/T_w} \tag{A4e}$$

The overall controllability factor can now be determined from the different contributions by the following equation

$$r_{\text{tot}} = mr = m_g m_f m_n m_d r_d r_{in} \qquad \text{(A4f)}$$

Equation A4f serves two purposes. The value of the overall controllability factor r_{tot} must be close to 1. As a rule of thumb values larger than 0.8 indicate good measurement/controller couples, while values below 0.5 indicate that control schemes are of little use. Equation A4f give us a quantity to directly compare various sensor/controller setups. The second advantage is that the overall uncertainty can be split up in separate contributions that can be optimized individually, with the aim of identifying (and ultimately removing) the bottleneck from a control structure or sensor implementation.

We would like to emphasize again that a more complete (English) treatment on the material as presented in this Appendix can be found in van der Grinten (1968).

Appendix B

The autonomous system in Eq. B1 serves as an example to study some of the influences of analyzer location and dynamics defined in the main text (van den Berg et al., 2000)

$$\dot{\boldsymbol{x}}(t) = \boldsymbol{A}_c\boldsymbol{x}(t) + \boldsymbol{b}_2 w(t) = \begin{bmatrix} -1 & 1 & 1.5 \\ 1 & -2 & 1 \\ 0 & 1 & -3 \end{bmatrix} \cdot \begin{bmatrix} x_1(t) \\ x_2(t) \\ x_3(t) \end{bmatrix} + \begin{bmatrix} 1 \\ 0 \\ 0 \end{bmatrix} \cdot w(t) \qquad \text{(B1)}$$

$$\boldsymbol{x}(0) = [1 \quad 1 \quad 1]' \qquad q(t) = 0.1$$

As can be seen from Eq. B1 disturbances $w(t)$ are "injected" on the first state and are distributed over the other two states

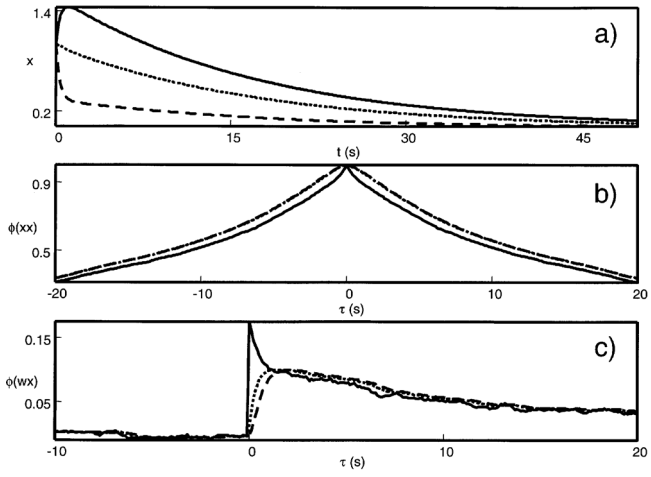

Figure B1. (a) Autonomous response; (b) auto- (c) and cross-correlation's for the three states in system (B.1): x_1(–), x_2(..) and x_3 (– –) (σ_{x1} = 0.17, σ_{x2} = 0.10 and σ_{x3} = 0.03).

Table BI. Three Different Analyzers for the System in Eq. B1

Analyzer	σ_i^2	T_g^*	T_i^*	T_f^*	T_d^*
B_a	1.0	—	—	0.1 s	—
B_b	0.1	—	—	5.0 s	5.0 s
B_c	0.5	—	2.0 s	0.1 s	—

* —means no significant contribution on the overall performance of this analyzer.

through the system dynamics in $\boldsymbol{A}_c$. The autonomous solution for the system plus the auto-correlation's $\phi(x_i x_i)$ and cross-correlation's $\phi(w_i x_i)$ for a white noise feed pattern with distribution $N(0, 0.1)$ is shown in Figure B1. The dynamics of state $x_1(t)$ and $x_2(t)$ show a clear system delay time for input uncertainty $w(t)$.

On this system, we define three 'instruments' with the specifications as shown in Table B1.

The specifications of the instruments imply the following characteristic features: B_a is a moderately accurate instrument with a high sampling frequency, B_b is a very accurate analyzer, however, it suffers from a large delay time (typically equal to the analysis time), and B_c is a representative of many physical measurements with a moderate accuracy and a significant memory effect.

Implementation of B_a is straightforward using the appropriate values in equations as presented in the theory section: sampling time T_f forms the basis for going from the continuous system in Eq. B1 to discrete observation, while σ_i^2 specifies the uncertainty in the measurement responses. To implement the time delay of B_b, measuring, for example, the first state, the original system $\boldsymbol{A}_c$ has to be augmented with three virtual states $x_4(t)$–$x_6(t)$ in accordance with Eq. 6 creating the *standard plant*

$$\dot{\boldsymbol{x}}(t) = \boldsymbol{A}_c\boldsymbol{x}(t) + \boldsymbol{b}_2 w(t)$$

$$= \begin{bmatrix} -1 & 1 & 1.5 & 0 & 0 & 0 \\ 1 & -2 & 1 & 0 & 0 & 0 \\ 0 & 1 & -3 & 0 & 0 & 0 \\ 1 & 0 & 0 & -2.4 & -2.4 & -0.96 \\ 0 & 0 & 0 & 1 & 0 & 0 \\ 0 & 0 & 0 & 0 & 1 & 0 \end{bmatrix} \cdot \begin{bmatrix} x_1(t) \\ x_2(t) \\ x_3(t) \\ x_4(t) \\ x_5(t) \\ x_6(t) \end{bmatrix} + \begin{bmatrix} 1 \\ 0 \\ 0 \\ 0 \\ 0 \\ 0 \end{bmatrix} \cdot w(t) \qquad \text{(B2)}$$

$$y(t) = \boldsymbol{c}'\boldsymbol{x} + v(t) = [-1 \quad 0 \quad 0 \quad 4.8 \quad 0 \quad 1.92]\boldsymbol{x} + v(t)$$

Table B11. Measurability Factors for the Analzyers in Table B1 Sampling the System in Eq. B1

Analyzer	x_1	x_2	x_3
B_a	0.8	0.7	0.3
B_b	0.4	0.3	0.1
B_c	0.7	0.6	0.4

In Eq. B2 the parameters for the augmented part of the system form a companion canonical state space representation of the Padé approximation for time delay in Eq. 6.

To model the signal correlation in B_c, sampling, for example, state number two, system $B1$ has to be augmented by one state $x_4(t)$ in accordance with Eq. 5

$$\dot{\boldsymbol{x}}(t) = \boldsymbol{A}_c\boldsymbol{x}(t) + \boldsymbol{b}_2 w(t)$$

$$= \begin{bmatrix} -1 & 1 & 1.5 & 0 \\ 1 & -2 & 1 & 0 \\ 0 & 1 & -3 & 0 \\ 0 & 1/2 & 0 & -1/2 \end{bmatrix} \cdot \begin{bmatrix} x_1(t) \\ x_2(t) \\ x_3(t) \\ x_4(t) \end{bmatrix} + \begin{bmatrix} 1 \\ 0 \\ 0 \\ 0 \end{bmatrix} \cdot w(t) \tag{B3}$$

$$y(t) = \boldsymbol{c}'\boldsymbol{x} + \sqrt{1-(e^{-1/T_i})^2} = [0 \quad 0 \quad 0 \quad 1]\boldsymbol{x} + 0.8v(t)$$

For these three analyzer types the uncertainty propagation from Eq. 9 is determined and the expected estimation error $\boldsymbol{P}_k$ is computed from Eqs. 7 and 8. The measurability factor Eq. 10 for these, the three analyzers in Table BI for the system B1, are given in Table BII. The table shows that measuring the first state is favorable for every instrument (van den Berg et al., 2000). It also shows that the best overall match between system and analyzer dynamics for state estimation is between B_a and the first state. The last conclusion from this example is that if only state x_3 is available, B_c is to be preferred.

Manuscript received Aug. 2, 1999, and revision received Mar. 19, 2001.